Grid-Based Distorted Born Approximation: A Dynamical Scattering Model for Coherent Surface Scattering Imaging

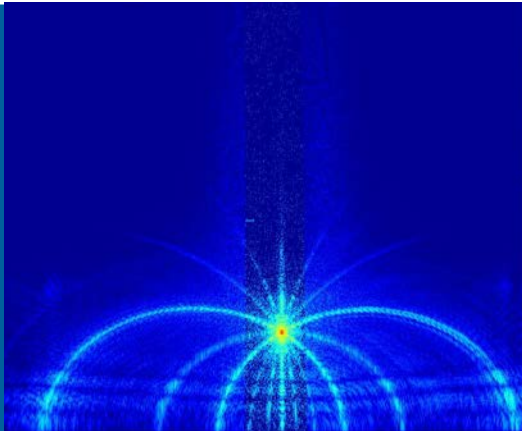

Miaoqi Chu, Zhang Jiang, Jin Wang
Advanced Photon Source
Argonne National Lab

September 13th, 2019 @ EBS-Workshop, ESRF Grenoble

Coherent Surface Scattering Imaging (CSSI)

Experiment geometry

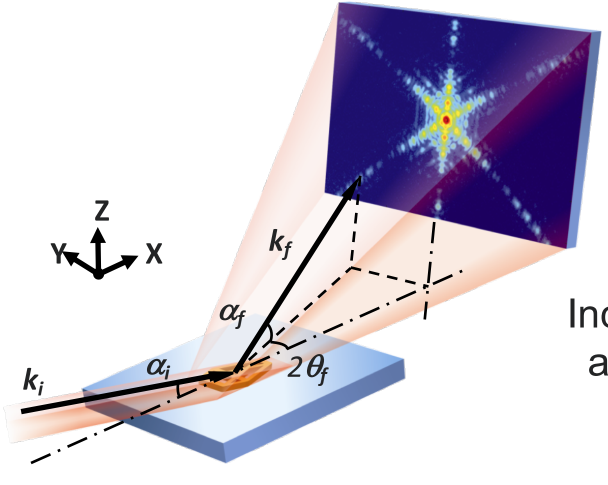

2D scattering patterns

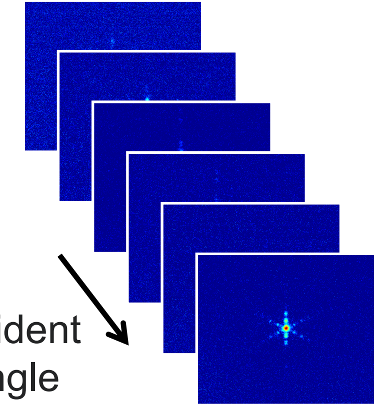

Incident angle

3D scattering data

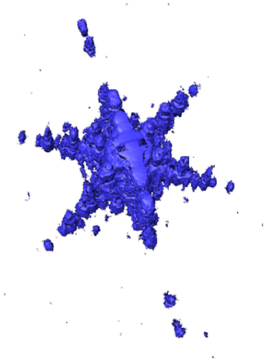

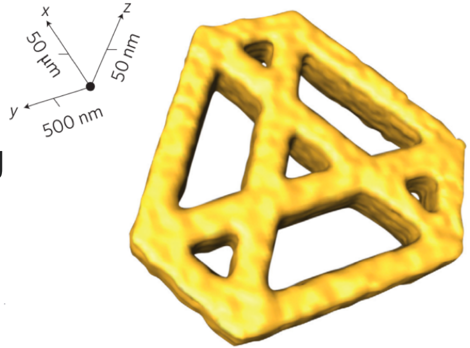

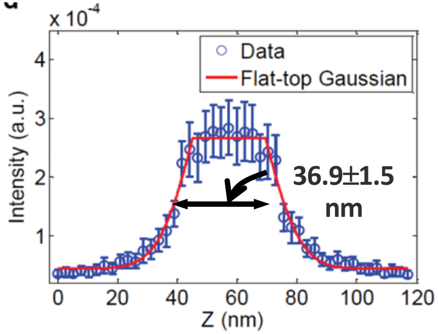

$$q_x = \frac{2\pi}{\lambda}(\cos(\alpha_f)\cos(2\theta_f) - \cos(\alpha_i))$$

$$q_y = \frac{2\pi}{\lambda}\cos(\alpha_f)\sin(2\theta_f)$$

$$q_z = \frac{2\pi}{\lambda}(\sin(\alpha_i) + \sin(\alpha_f))$$

Beamline: 8-ID-E at the APS

Beam energy: 7.35 keV

Beam size: 15 x 15 μm^2

Flux: ~10^9 photons/sec

Sample-to-detector: 0.7 m

Detector: Scintillator + Coolsnap HQ^2

5x lens (pixel dimension ~1.3 μm)

Incident angles: 0.35~0.9°

T. Sun, et al. Nature Photonics, 6, 586-590, 2012.

Probe extended objects with Ptychography

Translational scan the sample with a fixed beam; collect the scattering pattern at different locations.

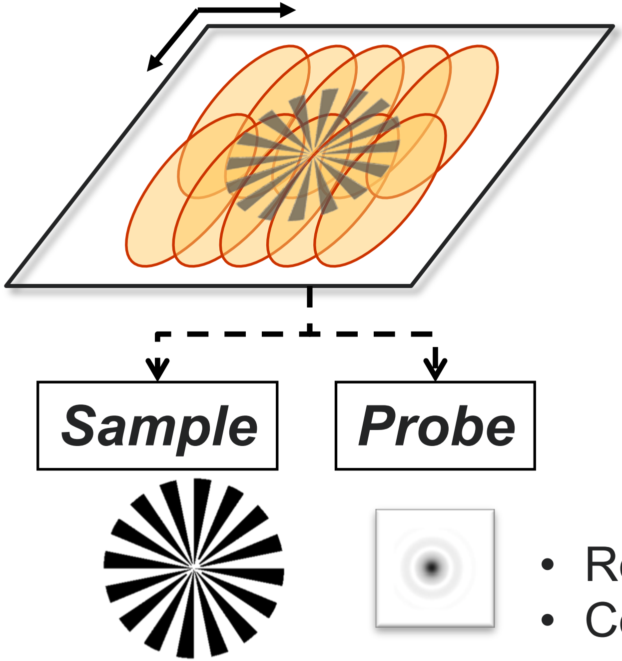

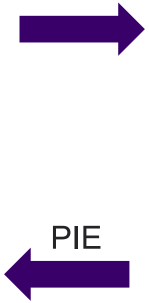

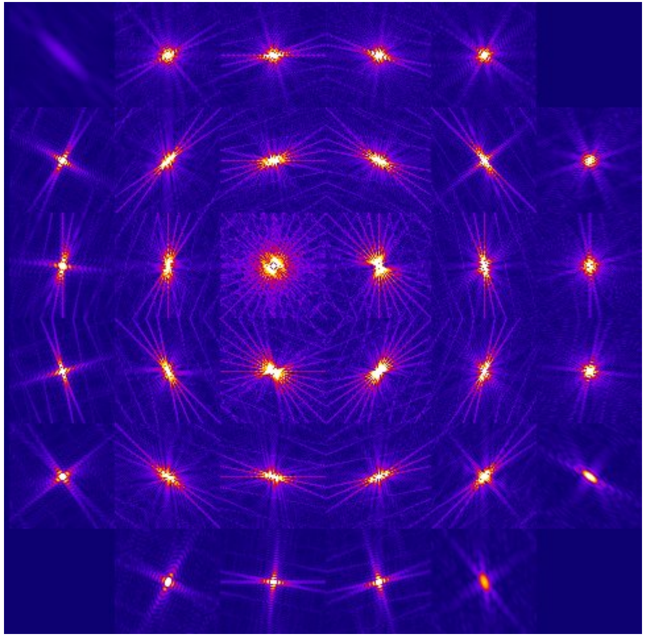

- Robust, relaxed constraint on the support and beam profile
- Combine with azimuthal rotation to achieve large area high-resolution (both x & y) imaging

CSSI features

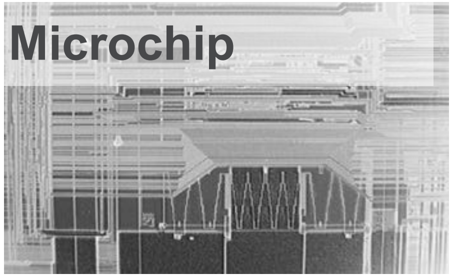

- ❖ Surface sensitive and depth-resolved
- ❖ Enhanced scattering at grazing incident angle.
- ❖ Large detection area
- ❖ No beam-stop: low-q accessibility
- ❖ High resolution:
  - ➢ x, y: ~5nm (through azimuthal rotation)
  - ➢ z: < 5nm
- ❖ A featured beamline of CSSI will be constructed for the APS-U.
  - APS upgrade to increase the coherent flux by 2-3 orders.
  - HPC resources from the Argonne Leadership Computing Facility (ALCF).
  - Many interesting science cases to be visited.
  - **30 Postdoc positions are available immediately; Contact Dr. Zhang Jiang (zjiang@anl.gov)**

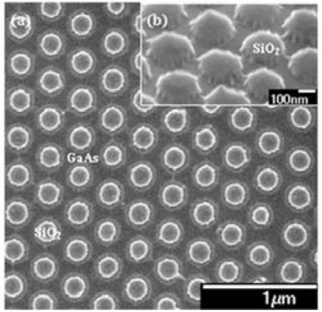

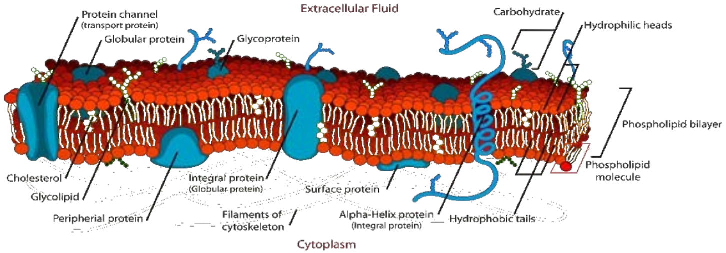

Fig1, wikipedia, biologydictionary.net, Tjahjana, Liliana, et al *Nanotechnology* 21.19 (2010): 195305.

Dynamical Scattering for surface scattering geometry

- Photons can be scattered more than once.
- Contains information about the sample
- Currently crop out during analysis.
- Require dynamical scattering theory beyond the Born approximation.

    - Gold bar on silicon surface
    - 70μm x 4μm x 50nm
    - Eiger 4M detector at 5m

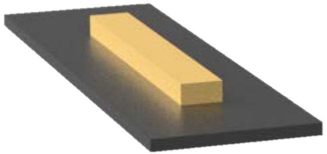

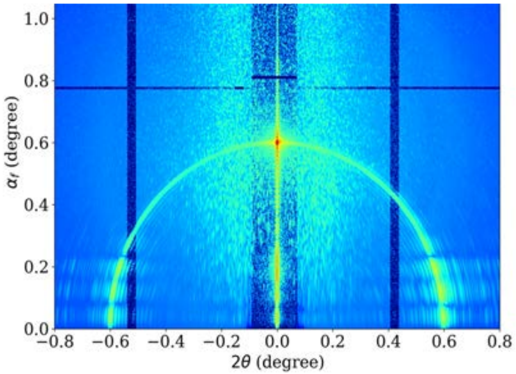

- Path
    - direct solve the Maxwell’s equations (Finite difference time domain etc)
    - **direct solve the scalar wave equation**

Helmholtz equation for scalar fields

X-ray propagation in medium can be simplified to the Helmholtz equation:

$$(\nabla^2 + k_0^2)\psi(\mathbf{r}) = U(\mathbf{r})\psi(\mathbf{r}), \qquad k_0 = 2\pi/\lambda \tag{1}$$

$$U(\mathbf{r}) = k_0^2(1 - n(\mathbf{r})^2) \approx 4\pi\rho(\mathbf{r}) \tag{2}$$

$n(\mathbf{r})$ is the refractive index, $n(\mathbf{r}) = 1 - \delta(\mathbf{r}) + i\beta(\mathbf{r}) = 1 - \frac{\lambda^2 r_e \rho(\mathbf{r})}{2\pi}$. The solution can be expressed in a Green's function integral (known as the Lippmann-Schwinger equation):

$$\psi(\mathbf{r}) = \phi(\mathbf{r}) + \int G_0(\mathbf{r}, \mathbf{r}')U(\mathbf{r}')\psi(\mathbf{r})d\mathbf{r}' \tag{3}$$

in which $\phi(\mathbf{r}), G_0(\mathbf{r}, \mathbf{r}')$ are solutions to

$$(\nabla^2 + k^2)[\phi(\mathbf{r}), G_0(\mathbf{r}, \mathbf{r}')] = [0, \delta^d(\mathbf{r}, \mathbf{r}')] \tag{4}$$

$$\phi(\mathbf{r}) = e^{i\mathbf{k}\cdot\mathbf{r}}, \qquad G_0(\mathbf{r}, \mathbf{r}')) = \frac{-1}{4\pi}\frac{e^{ik|\mathbf{r}-\mathbf{r}'|}}{|\mathbf{r} - \mathbf{r}'|} \tag{5}$$

Born Series and Born Approximation

The differential cross section between two states $\mathbf{k}_i$ and $\mathbf{k}_f$ can be reduced to

$$\frac{d\sigma}{d\Omega} = r_e^2 |\langle \phi_{\mathbf{k}_1}(\mathbf{r}) | \rho(\mathbf{r}) | \psi_{\mathbf{k}_2}(\mathbf{r}) \rangle|^2 \quad (6)$$

Solve Eq 3. self-consistently:

$$|\psi_{\mathbf{k}_2}(\mathbf{r})\rangle = |\phi_{\mathbf{k}_2}(\mathbf{r})\rangle + \hat{G}_0 \hat{U} |\phi_{\mathbf{k}_2}(\mathbf{r})\rangle + \hat{G}_0 \hat{U} \hat{G}_0 \hat{U} |\phi_{\mathbf{k}_2}(\mathbf{r})\rangle + \cdots \quad (7)$$

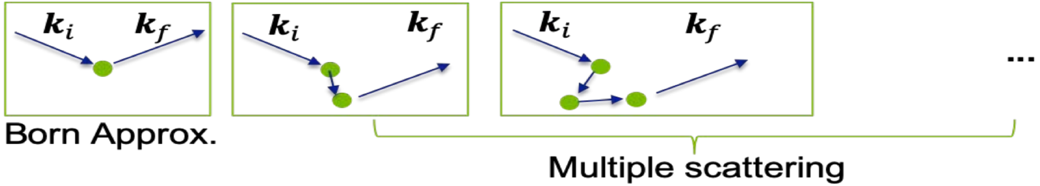

Born approximation

$$\frac{d\sigma}{d\Omega} = r_e^2 |\langle e^{i\mathbf{k}_1 \cdot \mathbf{r}} | \rho(\mathbf{r}) | e^{i\mathbf{k}_2 \cdot \mathbf{r}} \rangle|^2 = r_e^2 \left| \iiint \rho(\mathbf{r}) e^{-i\mathbf{q}\cdot\mathbf{r}} d\mathbf{r} \right|^2 \quad (8)$$

- In Born approximation, photons are scattered only once.
- Works for most weak scattering cases.
- Layered structures on the surface can be solved relatively easily.

Distorted Wave Born Approximation on a layered structure

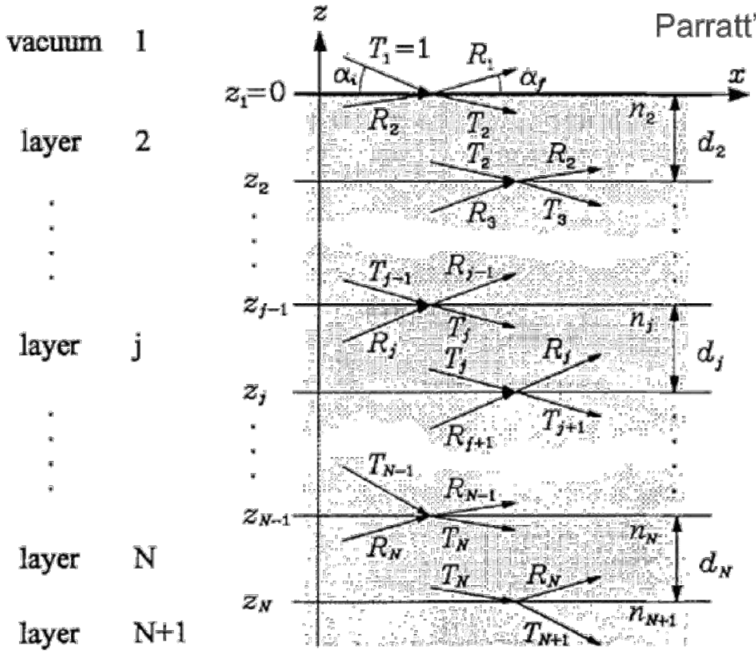

Figure: Ref: M. Tolan, X-Ray Scattering from Soft-Matter Thin Films (Springer, Berlin, 1999)

Parratt's Recursion

- Each layer has its own transmission and reflection, which distort the plane wave.

$$\psi_{j,\mathbf{k}}(\mathbf{r}) = e^{-i\mathbf{k}_{xy}\cdot\mathbf{r}_{xy}}\left(T_j e^{-ik_{z,j}z} + R_j e^{+ik_{z,j}z}\right)$$

- $T_0 = 1$ and $R_{N+1} = 0$
- Fresnel's equation is applied so that the boundary conditions are satisfied.
- This theory explains the total external reflection, and how X-ray mirrors work.

DWBA theory for Diffuse Surface Scattering by Sinha et al.

The sample is sliced into N layers; the electron density variation in each slice is minimized.

$$\bar{\rho}_j = \iint_S \rho(\mathbf{r}_{xy}, z_j) d\mathbf{r}_{xy}/S \qquad \delta\rho_j(\mathbf{r}) = \rho(\mathbf{r}) - \bar{\rho}_j \tag{9}$$

state 1: source $\rightarrow$ sample $\qquad \mathbf{k}^1 = (\mathbf{k}^1_{xy}, k^1_z)$ (10)

state 2: sample $\rightarrow$ detector (single pixel) $\qquad \mathbf{k}^2 = (\mathbf{k}^2_{xy}, k^2_z)$ (11)

$$|\psi_{j,\mathbf{k}_1}(\mathbf{r})\rangle = e^{-i\mathbf{k}^1_{xy}\cdot\mathbf{r}_{xy}}(T_j e^{-ik^1_{z,j}z} + R_j e^{+ik^1_{z,j}z}) \tag{12}$$

$$|\tilde{\psi}_{j,\mathbf{k}_2}(\mathbf{r})\rangle = e^{i\mathbf{k}^2_{xy}\cdot\mathbf{r}_{xy}}\left(T_j e^{-ik^2_{z,j}z} + R_j e^{+ik^2_{z,j}z}\right)^* \tag{13}$$

The total diffuse scattering cross section between the two states is:

$$\frac{d\sigma}{d\Omega} = \sum_{j=0}^{N} \left| \langle \tilde{\psi}_{j,\mathbf{k}_2}(\mathbf{r}) | \delta\rho(\mathbf{r}) | \psi_{j,\mathbf{k}_1}(\mathbf{r}) \rangle \right|^2 = r_e^2 \left| \sum_{m=1}^{m=4} \sum_{j=0}^{N} \int e^{-iq^m_{j,z}z} dz \iint D^m_j \delta\rho_j(\mathbf{r}) e^{-i\mathbf{q}^m_{j,xy}\cdot\mathbf{r}_{xy}} d\mathbf{r}_{xy} \right|^2$$

DWBA-Theory

$$\frac{d\sigma}{d\Omega} = r_e^2 \left| \sum_{m=1}^{4} \sum_{j=0}^{N-1} \iint D_j^m \, \delta\rho_j \, e^{-i\boldsymbol{q}_j^m \cdot \boldsymbol{r}} d\boldsymbol{r} \right|^2 = r_e^2 \left| \sum_{m=1}^{4} \sum_{j=0}^{N-1} \int e^{-iq_{j,z}^m z} dz \iint D_j^m \, \delta\rho_j \, e^{-i\boldsymbol{q}_{j,xy}^m \cdot \boldsymbol{r}_{xy}} dxdy \right|^2$$

$$D_j^1 = T_2^j T_1^j,$$

$$\boldsymbol{q}_j^1 = \boldsymbol{k}_j^2 - \boldsymbol{k}_j^1$$

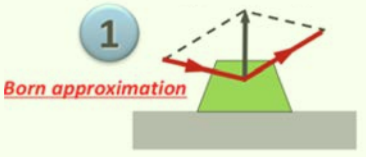

$$D_j^2 = R_2^j T_1^j,$$

$$\boldsymbol{q}_i^2 = \boldsymbol{k}_i^{2\prime} - \boldsymbol{k}_i^1$$

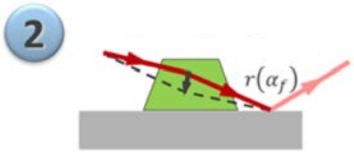

$$D_j^3 = T_2^j R_1^j,$$

$$\boldsymbol{q}_j^3 = \boldsymbol{k}_j^2 - \boldsymbol{k}_j^{1\prime}$$

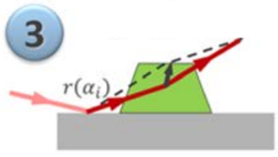

$$D_j^4 = R_2^j R_1^j,$$

$$\boldsymbol{q}_j^4 = \boldsymbol{k}_j^{2\prime} - \boldsymbol{k}_j^{1\prime}$$

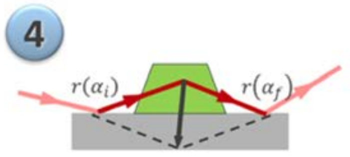

- DWBA takes the dynamical scattering effect in each layer into account, making the quantitative analysis of near-α_c scattering effect possible.
  - Eg. Reflectivity and Grazing incidence scattering.
- However, the DWBA theory requires the averaging of in-plane electron density:

$$\bar{\rho}^j = \frac{\iint \rho^j(x,y)dxdy}{\iint dxdy}, \quad \delta\rho^j(x,y) = \rho^j(x,y) - \bar{\rho}^j$$

- This averaging breaks down when the sample is highly heterogeneous on mesoscale.

Grid-DWBA

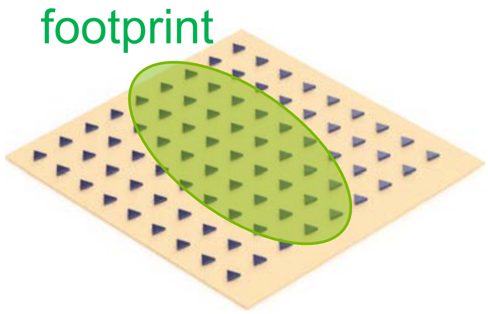

Beam footprint

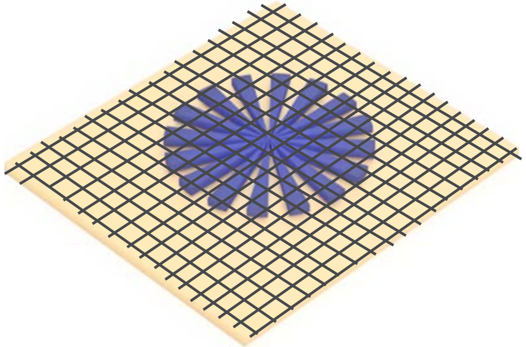

DWBA :

- One dimensional Electric field intensity modulation
- $\rho(z_n) = \frac{\iint \rho(x,y,z_n)dxdy}{\iint dxdy}$
- Works for weak perturbation

Grid-based DWBA:

- Three dimensional electric field intensity modulation
- Divide the whole sample area into (M_x, M_y) small (and thus more uniform) cells
- For the (i,j) th cell, centered at (x_{ij}, y_{ij})
  - $\rho_{ij}(z_n) = \frac{\iint \rho(x,y,z_n)dxdy}{\iint dxdy}$
- Calculate the EFI for each cell from $\rho_{ij}(z_n)$
- Calculate the diffuse scattering field in each cell and between nearby cells, add them with phase
- $I(\alpha_f, 2\theta) = |\sum_{i=0}^{M_x-1}\sum_{j=0}^{M_y-1} A_{ij}e^{i\phi_{ij}} + \sum_{Nearby} A_{ij\to i'j'}\, e^{i\phi_{ij}}|^2$

In-cells between cells

Example with only two cells

- The dynamical scattering from one cell can be scattered again by a nearby cell.

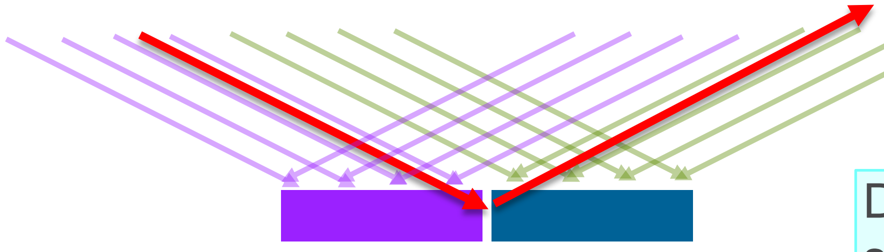

$$I = |A_P + A_Q + A_{PQ}|^2$$

Dynamical scattering in each cell

Dynamical scattering between nearby cells

$$A_P = r_e^2 \left| \sum_{m=1}^{4} \sum_{j=0}^{N-1} \iint D_{j,P}^{m}\, \delta\rho_j\, e^{-i\boldsymbol{q}_j^m \cdot \boldsymbol{r}} d\boldsymbol{r} \right|^2$$

$$D_{j,P}^1 = T_{2,P}^j T_{1,P}^j\,, \qquad D_{j,P}^2 = R_{2,P}^j T_{1,P}^j$$
$$D_{j,P}^3 = T_{2,P}^j R_{1,P}^j\,, \qquad D_{j,P}^4 = R_{2,P}^j R_{1,P}^j$$

$$A_{PQ} = r_e^2 \left| \sum_{m=1}^{4} \sum_{j=0}^{N-1} \iint D_{j,PQ}^{m}\, \delta\rho_j\, e^{-i\boldsymbol{q}_j^m \cdot \boldsymbol{r}} d\boldsymbol{r} \right|^2$$

$$D_{j,PQ}^1 = T_{2,P}^j T_{1,Q}^j\,, \qquad D_{j,PQ}^2 = R_{2,P}^j T_{1,Q}^j$$
$$D_{j,PQ}^3 = T_{2,P}^j R_{1,Q}^j\,, \qquad D_{j,PQ}^4 = R_{2,P}^j R_{1,Q}^j$$

Comparison between experiments and Grid-DWBA simulation

sample

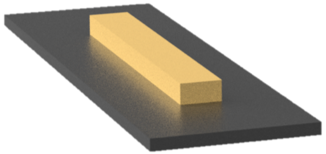

- Gold bar on silicon surface
- 70µm x 4µm x 50nm
- Eiger 4M detector at 5m

Lloyd's Mirror

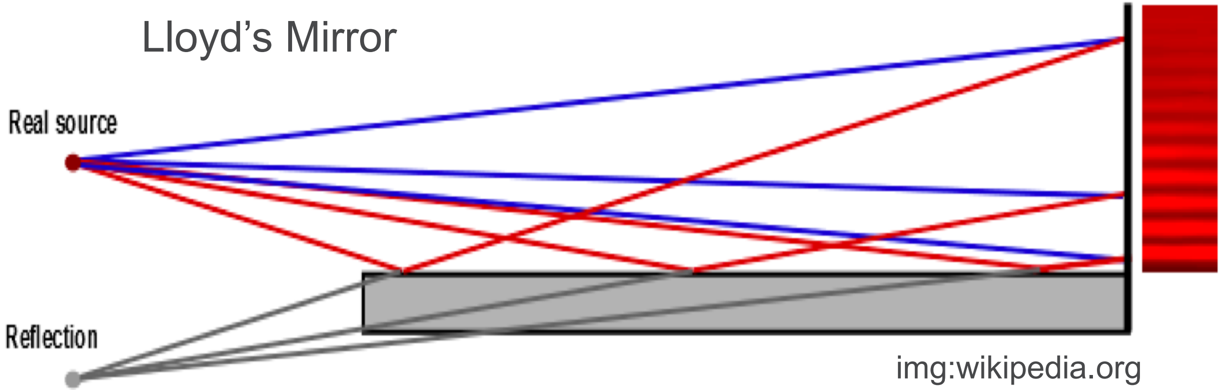

img:wikipedia.org

Experiment @ Petra III, 8keV

Grid - DWBA

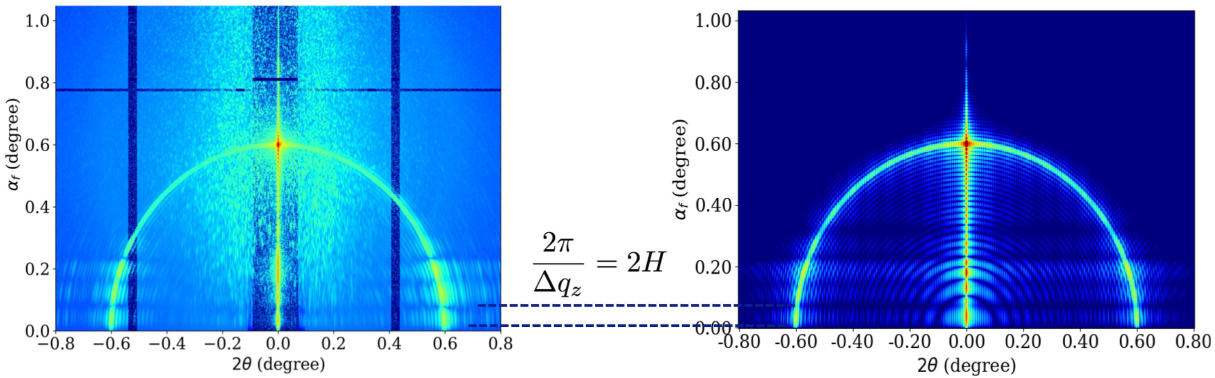

$$\frac{2\pi}{\Delta q_z} = 2H$$

Comparison between experiment and Grid-DWBA simulation

- Experiment performed at PetraIII
- 8.0keV, Eiger 4M @ 5.0m, $\alpha_i = 0.4\ deg$

3.5 µm x 350 µm x 50 nm (H)
Gold pattern on silicon

Experiment

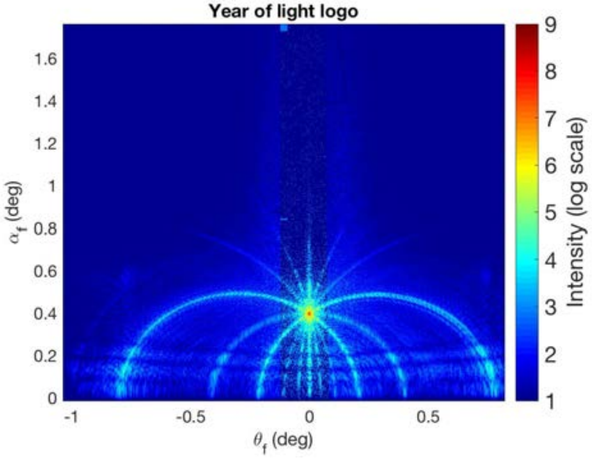

DWBA

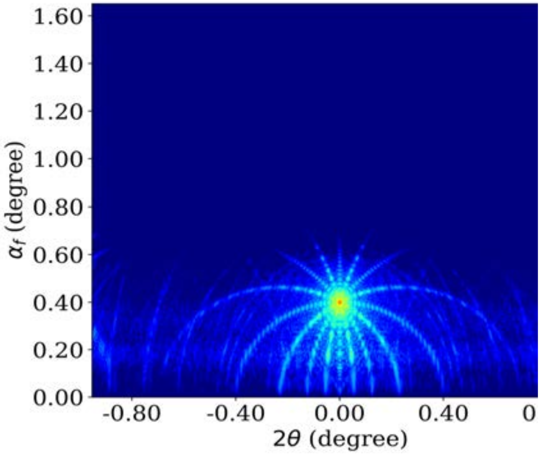

Grid-DWBA

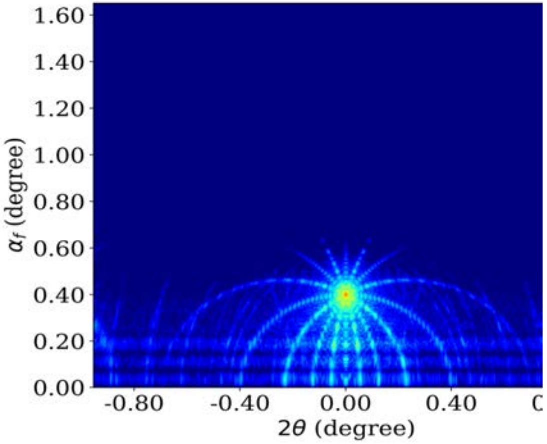

Case Study

- incident angle of 0.6 degree, 8 keV
- Effective scattering volume $= EE^{*}\rho(x, y)$

A silicon star on gold substrate

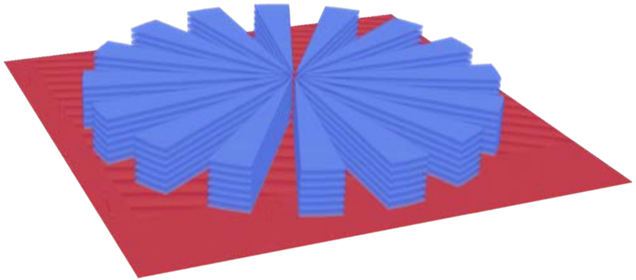

- X-rays penetrate the $\boldsymbol{H = 50nm}$ silicon, then reflected from the gold surface, creating standing wave inside silicon.
- The standing wave effect modulates the scattering pattern.

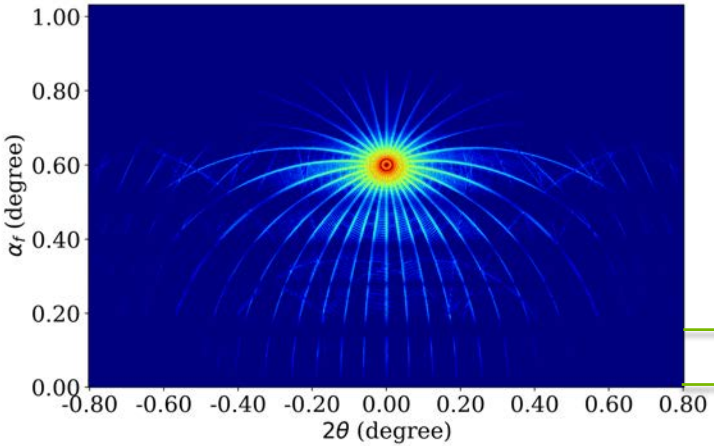

$$\frac{2\pi}{\Delta q_z} = H$$

A gold star on silicon substrate

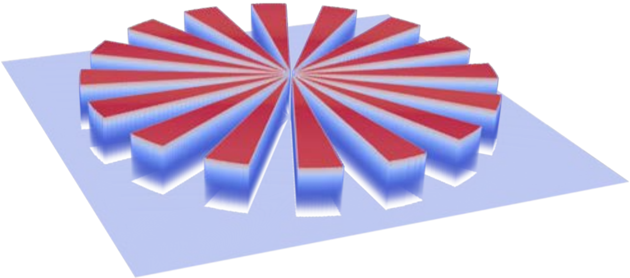

- The X-ray intensity decays as it enters the gold surface.
- The mixed term is relatively stronger than the previous case, introducing double-beating effect at low exit angle.

$$\frac{2\pi}{\Delta q_z} = 2H$$

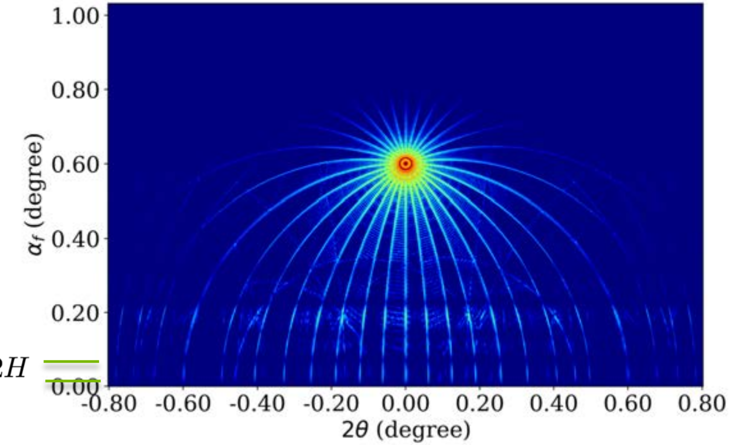

Summary

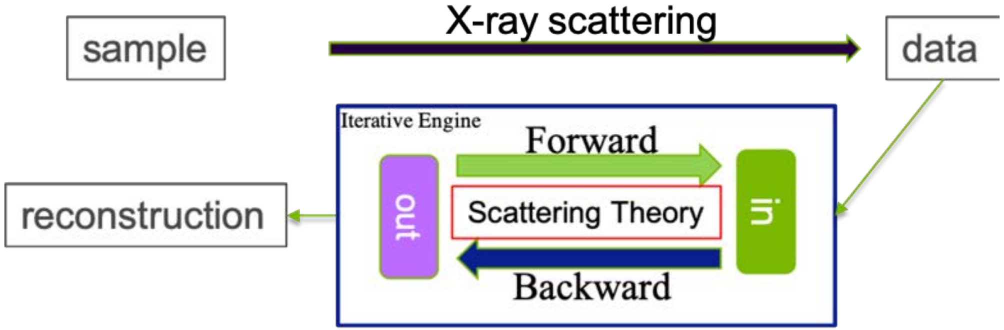

- Grid-based DBWA is able to capture the dynamical scattering effect in surface imaging setup.
- Scattering theories beyond the Born Approximation are required for
  - thick samples for ptychography
  - strong scattering objects for XPCI and CT
- We may have the computation power to implement dynamical scattering theories soon (now?).

name	speed Tflops (test)	fun fact
Earth Simulator (JPN)	35.86 (linpack)	fastest computer 2002-2004
Nvidia 2080Ti	0.43 (f64), 14.00 (fp32)	1,250 €, video gaming
Nvida V100	7.00 (fp64), 14.00 (fp32)	5,950 €, scientific computing
Aurora, Argonne	>1million (linpack)	commission 2021, user facility

QUESTIONS?